

A Frequency Domain Constraint for Synthetic X-ray Image Super Resolution

Qing Ma¹, Jae Chul Koh² and WonSook Lee¹

¹ University of Ottawa, Ottawa, Canada

¹ Korea University Anam Hospital, Seoul, Korea

{qma088, wslee}@uottawa.ca

Abstract. Synthetic X-ray images can be helpful for image guiding systems and VR simulations. However, it is difficult to produce high-quality arbitrary view synthetic X-ray images in real-time due to limited CT scanning resolution, high computation resource demand or algorithm complexity. Our goal is to generate high-resolution synthetic X-ray images in real-time by upsampling low-resolution images. Reference-based Super Resolution (RefSR) has been well studied in recent years and has been proven to be more powerful than traditional Single Image Super-Resolution (SISR). RefSR can produce fine details by utilizing the reference image but it still inevitably generates some artifacts and noise. In this paper, we propose texture transformer super-resolution with frequency domain (TTSR-FD). We introduce frequency domain loss as a constraint to further improve the quality of the RefSR results with fine details and without obvious artifacts. This makes a real-time synthetic X-ray image guided procedure VR simulation system possible. To the best of our knowledge, this is the first paper utilizing the frequency domain as part of the loss functions in the field of super-resolution. We evaluated TTSR-FD on our synthetic X-ray image dataset and achieved state-of-the-art results.

Keywords: Synthetic X-ray, Super Resolution, Frequency Domain, Digital Reconstructed Radiographs

1 Introduction

Efforts had been made on converting CT volume or slicing images into synthetic X-ray images, also known as Digital Reconstructed Radiographs (DRRs), with fast rendering algorithms such as ray tracing or ray casting methods [1–4]. In recent years, deep learning aided algorithms can generate highly realistic X-ray images but require vast training data and high computation resources [5, 6]. In general, there are three limitations to high-quality synthetic X-ray image generation. Firstly, it demands high computation resources to produce high-quality synthetic X-ray images, preventing the use in clinics or hospitals. Secondly, the algorithms for generating high-quality synthetic X-ray images are often time-consuming or complex. Finally, the resolution of the scan, i.e. the thickness of the scan, is not dense enough due to high dose radiation of CT scanning.

Each image of the CT scan can have high resolution, but the gap between slices is usually in a lot lower resolution. A basic requirement for generating adequate synthetic X-ray images is that the resolution is approximately equal in all directions [10]. For example, if a CT is scanned in the coronal view, the projected view on the sagittal view has a lot less resolution. Thus, it is necessary to up-sample the sagittal view, either with interpolation or more sophisticated methods such as semantic interpolation [11] or super-resolution.

Deep learning based Super-resolution has been widely applied for natural images. There are two main categories which are Single Image Super-Resolution (SISR) and Reference-based super-resolution (RefSR). SISR aims to reconstruct a high-resolution (HR) image from a single low-resolution (LR) image [12]. RefSR works on learning the high-resolution texture details from a given reference high-resolution image [13]. Convolution neural networks (CNN) and Generative adversarial network (GAN) methods have been widely used for SISR in recent years. However, CNN based super-resolution generates overly smooth images with coarse details. On the other hand, GAN based SR method generates appealing images with fine details but with more artifacts. This issue is especially crucial in medical imaging as image details have an impact on diagnosis and decision-making during operations. RefSR can learn fine texture details from the reference image but still generate some artifacts and noise. We propose to use a frequency domain loss as a constraint to mitigate this problem.

Various application scenarios have been explored with synthetic X-ray images. For example, arbitrary view synthetic X-ray images from CT data are used in virtual reality (VR) simulation for training medical doctors on fluoroscopy-guided intervention procedures [7, 8]. The VR simulation intends to replace real-life training sessions which is costly and exposed to radiation. High-quality DDRs can also be used as simulated X-Ray images for training datasets for machine learning approaches in Fluoroscopy-guided procedures [5]. It's also been found that using synthetic X-ray images can reduce up to half the amount of fluoroscopic images taken during real fluoroscopy-guided intervention procedures [9].

In this paper, we used a CPU based projection algorithm with a custom built lookup table created with tissue radiographic opacity parameters to generate fine low-resolution synthetic X-ray images from CT slices in an arbitrary view. And then, we use the state-of-the-art RefSR method combined with our frequency domain loss to generate a high-resolution synthetic X-ray image. We achieved state-of-the-art results on synthetic X-ray image super-resolution with our proposed TTSR-FD.

2 Related Work

SISR dedicate to learn the mapping between low-resolution and high-resolution images. Dong et al. [14] proposed SRCNN that first uses the deep learning method in SISR. It achieved superior results compared to previous conventional super-resolution methods. Another breakthrough made by Lim et al. [12] proposed EDSR introduced Residual Block into SISR. Zhang et al. [15] added the attention mechanism and proposed RCAN to further improve the network performance. These methods used CNN

yield a strong PSNR performance. However, they do not have a good visual quality as for human perceptions. GAN gradually become popular in this field of super-resolution research. Ledig et al. [16] proposed SRGAN first adopt GAN and showed appealing image quality. Wang et al. [17] introduced Residual-in-Residual Dense Block and relativistic GAN further improved the perceptual quality of the results.

RefSR takes advantage of learning more accurate details from the HR reference image. The reference image could be selected from adjacent frames in a video, images from web retrieval, an external database (dictionary), or images from different view-points [18]. It can achieve visually appealing results without generating many artifacts and noise compare to GAN based SISR. Zheng et al. [19] proposed CrossNet that adopts a flow-based cross-scale warping to transfer features. SRNTT [18] adopts patch matching with VGG extracted features and can use an arbitrary image as reference. Yang et al. [13] proposed TTSR applied a transformer network with attention models that achieved superior performance over traditional SISR methods. Nevertheless, these models still generate perceivable artifacts and noise in the resulting super-resolution synthetic X-ray image. The quality demand for medical images is higher.

Fourier transform is a powerful tool in the field of signal processing, and it has also shown great potential in deep learning related research. Rahaman et al. [20] adopt Fourier analysis that discovered empirical evidence shows low frequency is learned first by the network which is called the spectral bias. Li et al. [21] proposed the first neural network super-resolution method solely by learning in the frequency domain. It shows advantages on the speed of the model but with an imperceptible loss on result quality. Xu et al. [22] proposed a novel learning-based frequency channel selection method that achieved superior results on multiple tasks.

We made thoughtful analysis in the frequency domain for super-resolution and proposed a frequency domain loss to further improve the neural network performance. To the best of our knowledge, no previous works have tried utilizing a loss function in the frequency domain.

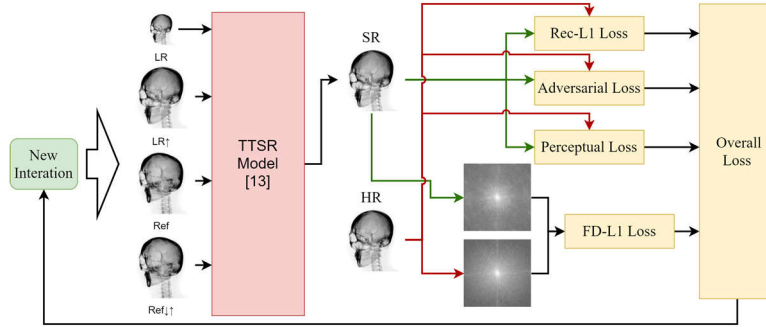


Fig. 1. Our super-resolution network, TTSR-FD. We add the frequency domain loss on the TTSR [13] model. The four input images are low resolution image (LR), up-sampled LR, reference images (Ref) and down/up-sampled Ref Image. Super resolution image (SR) is the model output. High resolution image (HR) is the ground truth image.

3 Methods

We aim to reduce the artifacts generated by the network while not losing the fine details. To achieve this, we introduce frequency domain loss as illustrated in Fig. 1. We explore the frequency domain pattern for different quality images in the magnitude spectrum. Then, we introduce our loss function in the frequency domain with Fourier transform.

3.1 Magnitude Spectrum for Images

We use the Fourier transform to see frequency patterns that are not obvious in the spatial domain. We check if the spectral bias is true for super-resolution [20]. We convert an input low-resolution image into a bicubic interpolated image, and several results of well-known super-resolution methods such as RCAN, ESRGAN, and TTSR. Their magnitude spectrums are shown in Fig. 2. While the bicubic interpolated image shows the worst results, we observe high-frequency details are not fully learned by any of the super-resolution models. We also show our TTSR-FD result as a comparison of the improvement.

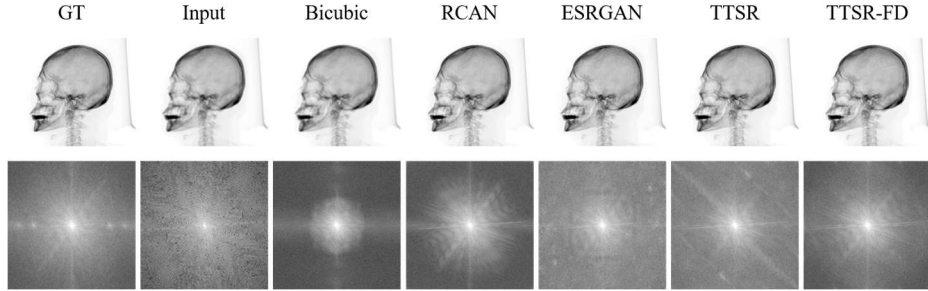


Fig. 2. Images in the magnitude spectrum where the first is the ground truth image, the second is the low-resolution input image and the last TTSR-FD is our result.

In general, we can see that we got whiter regions in the center showing images contain more low-frequency content. We can see from the input spectrum that it lost lots of high-frequency details compare to the GT. And the bicubic method is not able to generate high-frequency details. RCAN could only generate limited high-frequency details. ESRGAN can learn some good high-frequency details and shows sharp details in the spatial domain. But some odd patterns are shown in the frequency domain. There is a box shape rectangle in the center of the ESRGAN spectrum. We can see clearly from the spectrum that it is generating artifacts to satisfy human perceptual. TTSR can generate fine high-frequency details but also fails to match some patterns. Our TTSR-FD got the best spectrum similarity compared to the ground truth. We can find out that the frequency domain contains a lot of contents we do not have in the spatial domain.

3.2 Frequency Domain Loss

We introduce frequency domain loss based on the observation from the previous section. Our hypothesis is that a loss function in the frequency domain can increase the output image quality of RefSR. We aim to use this loss to set up a constraint during training that can force the model to learn more from the data and generate fewer artifacts and noise. We choose to build this constraint with a pixel-wise loss function to ensure the network can gain feedback on frequency domain patterns from the spectrum. We utilize $L1$ loss which is proven effective for super-resolution, also more robust and easier to converge compared to $L2$ loss. The general process of using frequency domain loss in our network is shown in Fig. 1. In short, we compute the loss by transfer model output and ground truth images of each iteration into frequency domain and calculate their $L1$ loss and feed back to the network. We applied this loss to our baseline model TTSR [13], which has three loss functions. The overall loss of the baseline model is:

$$\mathcal{L}_{overall} = \lambda_{rec}\mathcal{L}_{rec} + \lambda_{adv}\mathcal{L}_{adv} + \lambda_{per}\mathcal{L}_{per} \quad (1)$$

Where \mathcal{L}_{rec} is the reconstruction loss with $L1$ loss. \mathcal{L}_{adv} is the adversarial loss using WGAN-GP [23]. \mathcal{L}_{per} is the perceptual loss that include a normal perceptual loss and a texture wise loss [13]. λ is the weight coefficients for the loss functions. Below is the overall loss function of our model.

$$\mathcal{L}_{overall} = \lambda_{rec}\mathcal{L}_{rec} + \lambda_{fd}\mathcal{L}_{fd} + \lambda_{adv}\mathcal{L}_{adv} + \lambda_{per}\mathcal{L}_{per} \quad (2)$$

We added a frequency domain loss \mathcal{L}_{fd} to improve the network performance. In each iteration, a batch of SR and HR images are transferred into the frequency domain and then calculated their $L1$ loss.

$$S^{HR} = f_{rfft}(I^{HR}), \quad S^{SR} = f_{rfft}(I^{SR}) \quad (3)$$

$$\mathcal{L}_{fd} = \frac{1}{CHW} \|S^{HR} - S^{SR}\|_1 \quad (4)$$

Where I^{HR} and I^{SR} are high resolution and predicted super-resolution result images. S^{HR} and S^{SR} are the corresponding spectrum images after Fourier transform. C, H, W are the channel, height and width of the HR image. f_{rfft} represent the real-to-complex discrete Fourier transform function. We use real-to-complex discrete Fourier transform to improve the computation efficiency. There is no significant increase in time complexity of using our frequency domain loss during training.

4 Experiments

4.1 Datasets.

We created a reference-based super-resolution dataset for Synthetic X-ray images. The head CT data is provided by a Hospital (details hid). It contains seven different head CT series from five patients with Sagittal (SAG) and Coronal (COR) views. The

number of slices in these series ranges from 48 to 145 and each slice has 512x512 resolution. We used different variables for linear interpolation to fill the different sizes of gaps between slices for each series during the process of generating arbitrary views of synthetic X-ray images. Our projection method is built in Python with Numba.

We followed a similar approach described in SRNTT [18] to generate our dataset while making some adjustments considering the characteristic of synthetic X-ray images. In the training set, 225 (15x15) input images for each CT series are generated with a sampling step of 24 degrees for both x-axis and y-axis. The correspondence reference image is generated with a random range of rotation from -45 to 45 degrees. The training images are then cropped into five patches of 160x160 for each input image and reference image. We build a large training set SynXray_L consists of 1350 synthetic X-ray images with 512x512 resolution from four out of five patients and a small dataset SynXray_S consists of 410 synthetic X-ray images from three out of five patients. We choose to leave at least one patient out during training to make sure our test data is not seen during training. The test set X-ray images are randomly generated with a sampling step of 20 degrees. There are 30 images in the test set from all five patients.

4.2 Training Details

We used a similar training parameter setting as in TTSR [13]. We trained 50 and 100 epochs and pick the highest performance model for SynXray_L and SynXray_S dataset separately. We use a batch size of 4 and the learning rate is 1e-4 with Adam optimizer. The weight coefficient of the frequency domain loss is 0.01. We trained our network on upsampling factor x4 as it is a most likely scenario in real applications. We use PIL bicubic kernel for both downsampling and upsampling of input and reference images. We trained our model with a Tesla P100 GPU. The training time for large and small datasets is around 10 and 4 hours respectively.

4.3 Results

We compared our TTSR-FD with state-of-the-art methods, RCAN[15], ESRGAN[17] and TTSR[13]. TTSR as our base-line model has been made some minor modifications for training grayscale images by duplicate the grayscale channels. We evaluated our method on PSNR and SSIM as shown in Table 1. TTSR-FD achieved superior performance on both PSNR and SSIM. We also observe that TTSR-FD is strong on learning from a small dataset which indicates it can learn more from the data. This can be very beneficial for real-life applications since medical data are hard to obtain.

Table 1. PSNR/SSIM comparison among different SR methods on SynXray_S and SynXray_L datasets. The best results are in bold.

Method	SynXray S	SynXray L
RCAN	38.597/0.9482	38.880/0.9496
ESRGAN	34.483/0.9023	35.270/0.9140
TTSR	37.953/0.9393	38.115/0.9431
TTSR-FD (ours)	39.009/0.9521	39.261/ 0.9514

The best results are achieved at 60 and 70 epochs for TTSR and TTSR-FD on SynXray_S. We got the best performance at 10 and 20 epochs for TTSR and TTSR-FD on SynXray_L, respectively. We show the visual comparison for our method trained with SynXray_S on the test set in Fig. 3, considered that the visual difference between large and small datasets is minimal for our method. RCAN shows the second-highest accuracy in the quantitative measurement of PSNR and SSIM but we observe the image is overly smoothed and has limited high-frequency details. We can observe that the noise from the red circle area and black point artifacts from the rectangle area in TTSR have been removed in TTSR-FD. Our method can generate fine details without generating noise and artifacts.

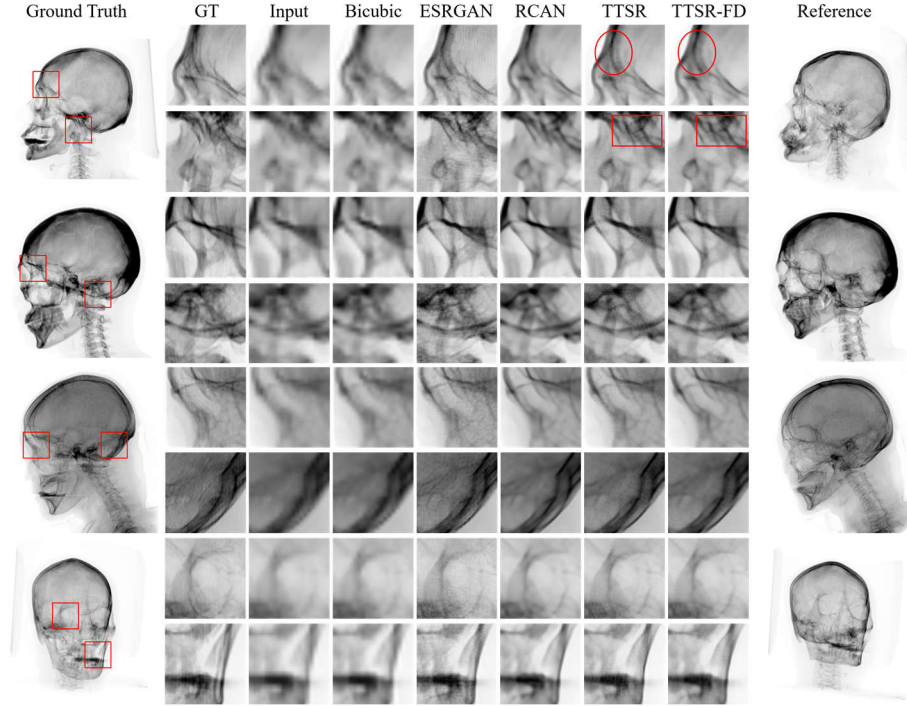


Fig. 3. Visual comparison for our method on testing set. Input Images are generated from SAG, SAG, SAG and COR view of CT data, respectively. TTSR-FD is ours.

4.4 Ablation study

In this section, we verify our proposed frequency domain loss is effective in improving model performance. We set up TTSR-Rec101 that has the same ratio of weight coefficients distribution as TTSR-FD where we increase the weight coefficients of reconstruction loss \mathcal{L}_{rec} from 1 to 1.01. We then compare it with our TTSR-FD model. The weight coefficients of TTSR-FD for \mathcal{L}_{rec} and \mathcal{L}_{fd} are 1 and 0.01. The weight

coefficients of other loss function \mathcal{L}_{adv} , \mathcal{L}_{per} are the same for both models. Our results are shown in Table 2.

Table 2. Ablation study for frequency domain loss with SynXray_S dataset

Method	PSNR	SSIM
TTSR	37.953	0.9393
TTSR-Rec101	38.245	0.9405
TTSR-FD	39.009	0.9521

We can see that compare to only increasing the reconstruction loss, the proposed frequency domain loss significantly improved the model performance. We also transfer our test images into magnitude spectrum to see the different patterns in frequency domain as shown in Fig. 4. We can see that without frequency domain loss, increasing the weight coefficient of the reconstruction loss could not improve the high-frequency details from the spectrum. We observed that the vertical line patterns that contain high-frequency details are not learned by TTSR-rec101 or TTSR as shown in red arrows.

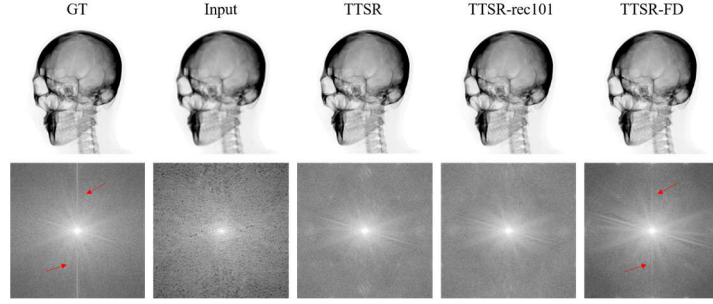


Fig. 4. Ablation study on frequency domain loss. Vertical line patterns indicated in red arrows in the ground truth image are only learned by TTSR-FD.

5 Conclusion

We proposed a texture transformer super-resolution with a frequency domain loss as a constraint for Synthetic X-ray image super-resolution. We demonstrate that an additional loss function in the frequency domain can improve the image quality for synthetic X-ray image super-resolution. Our work enables the possibility of generating high-quality synthetic X-ray images in real-time for Image Guiding Systems and VR simulations. Even though the experiments were done on synthetic X-ray images, the proposed method is applicable in other medical images. In future works, we would like to explore more possible loss variants and other application scenarios such as denoising in the frequency domain. It would be also interesting to see if the frequency domain loss can be helpful for natural image super-resolution as well.

References

1. Siddon, R.L.: Fast calculation of the exact radiological path for a three-dimensional CT array. *Medical physics*. 12, 252–255 (1985).
2. Jacobs, F., Sundermann, E., De Sutter, B., Christiaens, M., Lemahieu, I.: A fast algorithm to calculate the exact radiological path through a pixel or voxel space. *Journal of computing and information technology*. 6, 89–94 (1998).
3. Russakoff, D.B., Rohlfing, T., Mori, K., Rueckert, D., Ho, A., Adler, J.R., Maurer, C.R.: Fast generation of digitally reconstructed radiographs using attenuation fields with application to 2D-3D image registration. *IEEE transactions on medical imaging*. 24, 1441–1454 (2005).
4. Vidal, F.P., Garnier, M., Freud, N., Létang, J.-M., John, N.W.: Simulation of X-ray Attenuation on the GPU. In: *TPCG*. pp. 25–32 (2009).
5. Unberath, M., Zaech, J.-N., Lee, S.C., Bier, B., Fotouhi, J., Armand, M., Navab, N.: Deep-drr—a catalyst for machine learning in fluoroscopy-guided procedures. In: *International Conference on Medical Image Computing and Computer-Assisted Intervention*. pp. 98–106. Springer (2018).
6. Dhont, J., Verellen, D., Mollaert, I., Vanreusel, V., Vandemeulebroucke, J.: RealDRR—Rendering of realistic digitally reconstructed radiographs using locally trained image-to-image translation. *Radiotherapy and Oncology*. 153, 213–219 (2020).
7. Allen, D.R.: Simulation Approaches to X-ray C-Arm-based Interventions. 85.
8. Korzeniowski, P., White, R.J., Bello, F.: VCSim3: a VR simulator for cardiovascular interventions. *Int J CARS*. 13, 135–149 (2018). <https://doi.org/10.1007/s11548-017-1679-1>.
9. Touchette, M., Newell, R., Anglin, C., Guy, P., Lefaivre, K., Amlani, M., Hodgson, A.: The effect of artificial X-rays on C-arm positioning performance in a simulated orthopaedic surgical setting. *International Journal of Computer Assisted Radiology and Surgery*. 1–12 (2020).
10. Lin, E., Alessio, A.: What are the basic concepts of temporal, contrast, and spatial resolution in cardiac CT? *J Cardiovasc Comput Tomogr*. 3, 403–408 (2009). <https://doi.org/10.1016/j.jcct.2009.07.003>.
11. Li, J., Koh, J.C., Lee, W.-S.: Hrinet: Alternative Supervision Network For High-Resolution Ct Image Interpolation. In: *2020 IEEE International Conference on Image Processing (ICIP)*. pp. 1916–1920 (2020). <https://doi.org/10.1109/ICIP40778.2020.9191060>.
12. Lim, B., Son, S., Kim, H., Nah, S., Mu Lee, K.: Enhanced deep residual networks for single image super-resolution. In: *Proceedings of the IEEE conference on computer vision and pattern recognition workshops*. pp. 136–144 (2017).
13. Yang, F., Yang, H., Fu, J., Lu, H., Guo, B.: Learning Texture Transformer Network for Image Super-Resolution. *arXiv:2006.04139 [cs]*. (2020).
14. Dong, C., Loy, C.C., He, K., Tang, X.: Image super-resolution using deep convolutional networks. *IEEE transactions on pattern analysis and machine intelligence*. 38, 295–307 (2015).
15. Zhang, Y., Li, K., Li, K., Wang, L., Zhong, B., Fu, Y.: Image super-resolution using very deep residual channel attention networks. In: *Proceedings of the European conference on computer vision (ECCV)*. pp. 286–301 (2018).

16. Ledig, C., Theis, L., Huszár, F., Caballero, J., Cunningham, A., Acosta, A., Aitken, A., Tejani, A., Totz, J., Wang, Z.: Photo-realistic single image super-resolution using a generative adversarial network. In: Proceedings of the IEEE conference on computer vision and pattern recognition. pp. 4681–4690 (2017).
17. Wang, X., Yu, K., Wu, S., Gu, J., Liu, Y., Dong, C., Qiao, Y., Change Loy, C.: Esrgan: Enhanced super-resolution generative adversarial networks. In: Proceedings of the European Conference on Computer Vision (ECCV) Workshops. pp. 0–0 (2018).
18. Zhang, Z., Wang, Z., Lin, Z., Qi, H.: Image super-resolution by neural texture transfer. In: Proceedings of the IEEE/CVF Conference on Computer Vision and Pattern Recognition. pp. 7982–7991 (2019).
19. Zheng, H., Ji, M., Wang, H., Liu, Y., Fang, L.: Crossnet: An end-to-end reference-based super resolution network using cross-scale warping. In: Proceedings of the European conference on computer vision (ECCV). pp. 88–104 (2018).
20. Rahaman, N., Baratin, A., Arpit, D., Draxler, F., Lin, M., Hamprecht, F., Bengio, Y., Courville, A.: On the spectral bias of neural networks. In: International Conference on Machine Learning. pp. 5301–5310. PMLR (2019).
21. Li, J., You, S., Robles-Kelly, A.: A frequency domain neural network for fast image super-resolution. In: 2018 International Joint Conference on Neural Networks (IJCNN). pp. 1–8. IEEE (2018).
22. Xu, K., Qin, M., Sun, F., Wang, Y., Chen, Y.-K., Ren, F.: Learning in the frequency domain. In: Proceedings of the IEEE/CVF Conference on Computer Vision and Pattern Recognition. pp. 1740–1749 (2020).
23. Gulrajani, I., Ahmed, F., Arjovsky, M., Dumoulin, V., Courville, A.: Improved training of wasserstein gans. arXiv preprint arXiv:1704.00028. (2017).